lying on the curve of the sheaf corresponding to C = 1077. Thus a solution has been completely obtained in phase space. The dependence of the self-similar representations of the gas dynamic functions U, F, P on the self-similar variable ξ is defined ahead of the shock wave front by Eq. (2.2) and behind the front by Eq. (5.7).

Thus, the reflected shock wave front in the plane (r, t) corresponds to a line $\xi = \xi_f = -0.8809676$; ahead of the front $U_0 = -0.579504$, $F_0 = 0.181274$, $P_0 = 0.00869383$; behind the front $U_1 = 0.451876$, $F_1 = 0.304523$, $P_1 = 0.0524506$. The gas dynamic function distribution on the focus section is as follows: $u = 0.82318\ \xi_0 r^{1-k}$, $c^2 = 0.115196\ \xi_0^2 r^{2(1-k)}$, $p = 0.0463816\ \xi_0^4 r^{3-4k}$, $\rho = 0.671053\ \xi_0^2 r^{1-2k}$. The change with time in gas dynamic functions at the center is $u(0, t) = 0$, $p(0, t) = 1.524038 \cdot 10^{-6} |\xi_0|^{3/k} t^{3/k-4}$, $c^2(0, t) = 0.00028086\ |\xi_0|^{2/k} t^{2(1-k)/k}$, $\rho(0, t) = 0.009043\ |\xi_0|^{1/k}\ t^{1/k-2}$.

The authors are deeply indebted to V. S. Imshennik for posing the problem studied and evaluating the results obtained and to M. S. Gavreeva for clerical assistance.

LITERATURE CITED

1. K. V. Brushlinskii and Ya. M. Kazhdan, "Self-similar solutions of some gas dynamics problems," Usp. Mat. Nauk, 18, No. 2 (110), (1963).
2. Ya. B. Zel'dovich and Yu. P. Raizer, Physics of Shock Waves and High Temperature Hydrodynamic Phenomena [in Russian], Fizmatizdat, Moscow (1963).
3. I. B. Shchenkov, SANTRA Symbol-Analytic Transform System. Input Language, Preprint Inst. Prikl. Mat. No. 19 [in Russian], Moscow (1987).

BOUNDARY CONDITIONS ON A SHOCK WAVE IN A SUPERSONIC FLOW

V. G. Shcherbak

UDC 533.6.011

The theory in [1, 2] is used extensively in investigations of supersonic viscous gas flow around blunt bodies. A two-layer flow model consisting of a viscous shock layer and a domain of passage through the compression shock is proposed in these papers on the basis of an analysis of plane and axisymmetric supersonic flows around bodies.

The equations describing the domain of passage through the shock are integrated once and the relationships obtained (generalized Rankine—Hugoniot conditions) are used as boundary conditions on the outer boundary of the viscous shock layer. In contrast to the classical Rankine—Hugoniot conditions, the generalized conditions take account of molecular transport effects in the zone of the compression shock. The question of the influence of viscosity and heat conductivity on the flow of a homogeneous gas behind a strongly curved shockwave was first investigated in [3].

When chemical reactions are present in the flow, the problem of flow in a shock layer is already, in principle, not separated from the problem of the shockwave structure because of the presence of a source term in the mass conservation laws of the separate components. To compute it in the generalized Rankine—Hugoniot relationships the problem of the shockwave structure must be solved and joined with the solution within the shock layer. Avoiding this procedure to close the problem on the viscous shock layer, the chemical reactions within the shockwave are neglected by omitting the source term in the boundary conditions. As is shown in [4], let us note that the modified Rankine—Hugoniot relationships should be utilized for large Reynolds numbers; also sine application of the ordinary Rankine—Hugoniot relationships results in a finite error in the general case because of the origination of a source (sink) of the chemical component on the boundary.

The approximate analytic estimates executed in [5] showed that the two-layer model with the frozen wave front is justified for air for $V_\infty \leqslant 7$ km/sec. It is interesting to estimate numerically the influence of chemical reactions in the shock leading front on the flow characteristics.

Moscow. Translated from Zhurnal Prikladnoi Mekhaniki i Tekhnicheskoi Fiziki, No. 1, pp. 49-56, January-February, 1989. Original article submitted October 6, 1987.

1. Formulation of the Problem

Let us consider the flow around a smoothly blunt body. Let us introduce a certain arbitrary curvilinear coordinate system coupled normally to the streamlined surface. Let $x^3 = \text{const}$ be the equation of a family of surfaces parallel to the body surface, and $x^3 = 0$, x^1, x^2 are selected on the surface. We shall start from the simplified Navier—Stokes equations in which terms comprising the Euler equation, the second-approximation boundary layer equations, the terms describing the shockwave structure in a supersonic approximation [6] and certain other terms are retained. Taking account of nonequilibrium chemical reactions, multicomponent diffusion, and barodiffusion and neglecting thermal diffusion, the equations in the coordinate system $\{x^i\}$ have the following dimensionless form

$$\frac{\partial}{\partial x^i}\left(\rho u^i \sqrt{\frac{g}{g_{(ii)}}}\right) = 0, \quad g_{33} = 1, \quad g_{3\alpha} = g_{\alpha 3} = 0; \tag{1.1}$$

$$\rho Du^\alpha + \rho A^\alpha_{\beta\gamma} u^\beta u^\gamma + \{2\rho A^\alpha_{\beta 3} u^\beta u^3\} = -\sqrt{g_{(\alpha\alpha)}}\, g^{\alpha\beta}\frac{\partial p}{\partial x^\beta} + \sqrt{\frac{g_{(\alpha\alpha)}}{g}}\frac{\partial}{\partial x^3}\left(\frac{\mu\sqrt{g}}{\mathrm{Re}_\infty}\frac{\partial u^\alpha/\sqrt{g_{(\alpha\alpha)}}}{\partial x^3}\right), \quad \alpha = 1, 2; \tag{1.2}$$

$$\{\rho Du^3\} + \rho A^3_{jk} u^j u^k = -\frac{\partial p}{\partial x^3} + \left\{\frac{4}{3}\frac{1}{\sqrt{g}}\frac{\partial}{\partial x^3}\left(\frac{\mu\sqrt{g}}{\mathrm{Re}_\infty}\frac{\partial u^3}{\partial x^3}\right)\right\}; \tag{1.3}$$

$$\rho c_p DT = \frac{1}{\sqrt{g}}\frac{\partial}{\partial x^3}\left(\frac{\mu c_p\sqrt{g}}{\mathrm{Re}_\infty \sigma}\frac{\partial T}{\partial x^3}\right) + \frac{\mu g_{\alpha\beta}}{\mathrm{Re}_\infty}\frac{\partial u^\alpha/\sqrt{g_{(\alpha\alpha)}}}{\partial x^3}\frac{\partial u^\beta/\sqrt{g_{(\beta\beta)}}}{\partial x^3} - \tag{1.4}$$

$$-\sum_{i=1}^{N} h_i \dot{w}_i - \left(\sum_{i=1}^{N} c_{pi} I_i\right)\frac{\partial T}{\partial x^3} + \frac{u^\alpha}{\sqrt{g_{(\alpha\alpha)}}}\frac{\partial p}{\partial x^\alpha} + \left\{u^3\frac{\partial p}{\partial x^3} + \frac{4}{3}\frac{\mu}{\mathrm{Re}_\infty}\left(\frac{\partial u^3}{\partial x^3}\right)^2\right\};$$

$$\rho Dc_i + \frac{1}{\sqrt{g}}\frac{\partial\sqrt{g}\, I_i}{\partial x^3} = \dot{w}_i, \quad i = 1, \ldots, N - Ne,$$

$$\rho Dc_k^* + \frac{1}{\sqrt{g}}\frac{\partial\sqrt{g}\, I_k^*}{\partial x^3} = 0, \quad k = 1, \ldots, Ne - 1,$$

$$\frac{\mu}{\mathrm{Re}_\infty}\frac{\partial x_i}{\partial x^3} = \sum_{j=1}^{N}\frac{m^2}{m_i m_j} S_{ij}(c_i I_j - c_j I_i) - \left\{\frac{\mu}{\mathrm{Re}_\infty} x_i\left(1 - \frac{m_i}{m}\right)\frac{\partial \ln p}{\partial x^3}\right\},$$

$$p = R_G \rho\frac{T}{m}, \quad \sum_{k=1}^{Ne} I_k^* = 0, \quad \sum_{k=1}^{Ne} c_k^* = 1, \quad m = \left(\sum_{i=1}^{N}\frac{c_i}{m_i}\right)^{-1},$$

$$c_p = \sum_{i=1}^{N} c_i c_{pi}, \quad x_i = \frac{c_i m}{m_i}, \quad D = \frac{u^\alpha}{\sqrt{g_{(\alpha\alpha)}}}\frac{\partial}{\partial x^\alpha} + u^3\frac{\partial}{\partial x^3},$$

$$g_{\alpha\beta} = a_{\alpha\beta} - 2b_{\alpha\beta}x^3 + a^{\gamma\lambda}b_{\gamma\alpha}b_{\lambda\beta}(x^3)^2, \quad g = \det\|g_{ij}\|,$$

$$A^i_{jk} = \frac{1}{2\sqrt{g_{(jj)}g_{(kk)}}}\left[\sqrt{g_{(ii)}}\, g^{il}\left(\frac{\partial g_{kl}}{\partial x^j} + \frac{\partial g_{jl}}{\partial x^k} - \frac{\partial g_{jk}}{\partial x^l}\right) - \delta^i_j\frac{\partial\sqrt{g_{(jj)}}}{\partial x^k} - \delta^i_k\frac{\partial\sqrt{g_{(kk)}}}{\partial x^j}\right]. \tag{1.5}$$

Here summation is over a pair of identical subscripts, there is no summation over the subscripts enclosed by parentheses; unless especially stipulated otherwise, the Latin subscripts take on the values 1, 2, 3 and the Greek the values 1 and 2; $a_{\alpha\beta}$, $b_{\alpha\beta}$ are covariant components of symmetric tensors governing the first and second quadratic forms of the surface, respectively; $V_\infty u^i$ are physical components of the velocity vector corresponding to the axes x^1, x^2, x^3; $\rho_\infty V_\infty^2 p$, $\rho_\infty \rho$, $T_0 T$ are the pressure, density, and temperature of the gas mixture consisting of N chemical components ($T_0 = V_\infty^2/c_{p\infty}$); $\mu_\infty\mu$, $c_{p\infty}c_p$, Re_∞, σ, m are the viscosity coefficient, specific heat, Reynolds and Prandtl numbers, and the molecular mass of the mixture; c_i, m_i, $c_{p\infty}T_0 h_i$, $c_{p\infty}c_{pi}$, $\rho_\infty V_\infty I_i$, $\rho_\infty V_\infty w_i/R$ are the mass concentration, molecular mass, specific enthalpy and heat, normal component of the diffusion flux vector, rate of mass formation of the i-th component; c_k^*, $\rho_\infty V_\infty I_k^*$ are the concentration and normal component of the diffusion flux vector of the k-th element; Ne is the number of elements; S_{ij} (i, j = 1, ..., N) are binary Schmidt numbers; $c_{p\infty}R_G$ is the universal gas constant; and V_∞ is the modulus of the incoming stream velocity vector. All the linear dimensions are referred to the characteristic linear dimension R which is the bluntness radius of curvature. Here and henceforth, the subscripts ∞, w, s are referred to parameters in the incoming stream, on the body surface, and on the inner shockwave boundary.

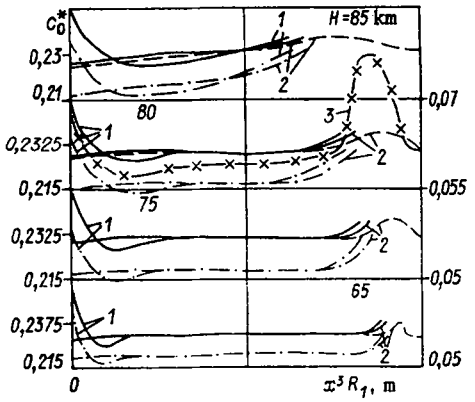

Fig. 1

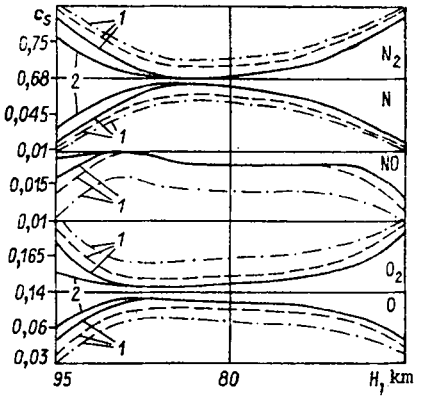

Fig. 2

If terms in the braces are omitted, then we obtain a system of thin viscous shock layer equations [7] in which the space metric is taken completely into account including terms out of order (in [7] it is assumed $g_{\alpha\beta} = a_{\alpha\beta}$). Let us designate the system (1.1)-(1.5) the system I, and the equations with the terms in braces omitted the system II.

Neglecting slip, temperature and concentration jumps, the boundary conditions on the body surface are as follows:

$$x^3 = 0, \quad u^\alpha = u^3 = 0, \quad q = \Gamma T^4, \quad \Gamma = \varepsilon\sigma_B T_0^4/(\rho_\infty V_\infty^3),$$
$$I_i = -\rho k_{wi} c_i, \quad i = 1, \ldots, N - Ne, \quad I_k^* = 0, \quad k = 1, \ldots, Ne - 1,$$

where ε is the surface emissivity, σ_B is the Stefan—Boltzmann constant, and $V_\infty k_{wi}$ is the heterogeneous recombination rate constant.

Conditions corresponding to incoming stream parameters are given on the outer boundary for the system I. For the system II generalized Rankine—Hugoniot relations are given as boundary condition on the shockwave, and which have the following form in a supersonic approximation when chemical reactions within the shockwave are neglected

$$\rho\left(u^3 - \frac{u^\alpha}{\sqrt{g_{(\alpha\alpha)}}}\frac{\partial x_s^3}{\partial x^\alpha}\right) = u_\infty^3, \quad u_\infty^3 (u^\alpha - u_\infty^\alpha) = \frac{\mu}{\mathrm{Re}_\infty}\sqrt{g_{(\alpha\alpha)}}\frac{\partial u^\alpha/\sqrt{g_{(\alpha\alpha)}}}{\partial x^3},$$

$$u_\infty^3\left(H - H_\infty - \frac{(u_\infty^3)^2}{2}\right) = \frac{\mu c_p}{\sigma\,\mathrm{Re}_\infty}\frac{\partial T}{\partial x^3} - \sum_{k=1}^{N} h_i I_i + \frac{\mu}{\mathrm{Re}_\infty} B_{\alpha\beta}\sqrt{g_{(\alpha\alpha)}}\frac{\partial u^\alpha/\sqrt{g_{(\alpha\alpha)}}}{\partial x^3}u^\beta, \tag{1.6}$$

$$p = (u_\infty^3)^2, \quad H = h + \frac{1}{2}B_{\alpha\beta}u^\alpha u^\beta, \quad B_{\alpha\beta} = \frac{g_{\alpha\beta}}{\sqrt{g_{(\alpha\alpha)}g_{(\beta\beta)}}};$$

$$u_\infty^3 (c_k^* - c_{k\infty}^*) + I_k^* = 0, \quad k = 1, \ldots, Ne - 1; \tag{1.7}$$

$$u_\infty^3 (c_i - c_{i\infty}) + I_i = 0, \quad i = 1, \ldots, N - Ne. \tag{1.8}$$

The presence of the components N_2, O_2, N, O, NO between which dissociation—recombination and exchange reactions proceed in the perturbed flow domain, is assumed when examining the chemical reactions. The system of reactions, the reaction rate constants, and the transport coefficient agree with those utilized in [7]. The assumption is used that the internal degrees of freedom are excited in equilibrium.

2. On the Method of Solving the Problem Numerically

We assume that the equation of the body surface in the neighborhood of the stagnation point can be approximated to second order accuracy by the equation of an elliptical paraboloid $2y^3 = (y^1)^2 + k(y^2)^2$, $k = R_1/R_2$ (R_1 and R_2 are the radii of principal curvature of the surface at the stagnation point and $\{y^i\}$ is a Cartesian coordinate system connected to the stagnation point).

Dorodnityn variables [8] and new functions

$$\xi^\alpha = x^\alpha, \quad \eta = \frac{1}{\Delta}\int_0^{x^3} \rho \sqrt{g}\, dx^3, \quad u^\alpha = d_{(\alpha)}\xi^{(\alpha)} \sqrt{g_{(\alpha\alpha)}}\, \frac{\partial \varphi_\alpha}{\partial \eta^3}$$

$$\rho \sqrt{g}\, u^3 = -\frac{\partial \left[\Delta d_{(\alpha)}\xi^{(\alpha)}\varphi_\alpha\right]}{\partial \xi^\alpha} - \Delta d_{(\alpha)}\xi^{(\alpha)} \frac{\partial \varphi_\alpha}{\partial \eta}\frac{\partial \eta}{\partial x^\alpha}, \quad d_1 = 1, \quad d_2 = k \tag{2.1}$$

are introduced for the numerical solution of the problem. The continuity equation for the mixture is here satisfied identically.

The system I was solved on the stagnation line within the framework of a local self-similar approximation of the Navier—Stokes equations [9]. The desired solution was represented in the form of series. Substituting the expansion in the system I and applying the procedure for truncating series [10], we obtain a system of ordinary differential equations for the zeroth terms of the expansion and equations to determine the pressure gradients. The density was found from (1.3), and the pressure from the equation of state. The mesh was concentrated in the shockwave domains (according to the profile $1/\rho$) and the boundary layer domains (according to the enthalpy profile) so that they contained not less than 5-7 nodes.

Going over to the variables (2.1) in the system II resolves all singularities that occur in the coefficients of the equations at the stagnation point. A system of ordinary-differential equations is here obtained in which the pressure gradients were determined from (1.3) (with terms in the braces omitted) after the operator $(d_{(\alpha)}\xi^{(\alpha)})^{-1}\partial/\partial\xi^\alpha$ has been applied, the pressure itself from (1.3) of system II, the density from the equation of state. For the system II $\Delta = \int_0^{x_s^3} \rho \sqrt{g}\, dx^3$ (found during solution of the problem), and for the system I $\Delta = 1$.

A scheme [11] having four orders of accuracy in the transverse coordinate was utilized for the numerical solution. Simple iterations were performed to overcome the nonlinearity of the equations. A more detailed description of the methods for solving the systems I and II is presented in [7, 9].

3. Analysis of the Numerical Results

Let us consider the motion of a body along an earth re-entry trajectory [12] (line 7 in Fig. 4), which is assumed isothermal with a density distribution from the altitude H (km) $\rho_\infty = 1.225 \cdot 10^{-3} \exp(-0.142\ H)$ g/cm^3 and $T_\infty = 250$ K. The results of computations in the neighborhood of the stagnation point at which the smaller of the radii of curvature is $R_1 = 0.5$ m, $k = 0.4$, $\varepsilon = 0.85$, are presented below.

The influence of catalytic surface properties, multicomponent diffusion, and barodiffusion on the concentration profile for the oxygen element is shown in Fig. 1 for different points of the trajectory. The solid lines are the solution of the system II and the dashes of the system I without taking barodiffusion into account. Lines 1 and 2 in Figs. 1 and 2 correspond to ideally catalytic and non-catalytic surfaces.

At the altitudes $H \geqslant 85$ km the shockwave and shock layer thicknesses are of the same order and the molecular transport effects are substantial in all the perturbed flow domains, a change in the surface catalytic properties results in a change in the whole concentration profile. As the flight altitude diminishes an inviscid flow domain starts to be formed in which separation of the chemical elements is independent of the catalytic properties of the surface in practice. In the viscous near-wall domain the element constitution depends substantially on the heterogeneous reaction progress model. The shock layer thickness for equilibrium reactions on the surface is less than for frozen reactions. As the flight altitude ($H < 65$ km) and the boundary layer thickness diminish, the influence of the surface catalysis on the stand-off practically vanishes.

Comparison of the results of computations of a thin viscous shock layer with the simplified Navier—Stokes equations shows that the concentration profiles agree well with the exception of a domain abutting on the shockwave, and the shockwave stand-off in the thin viscous shock layer model is smaller.

Neglecting the diffusion flux in the boundary conditions for the concentration (the dash-dot lines) results in a reduction in the fraction of the element O, where the difference

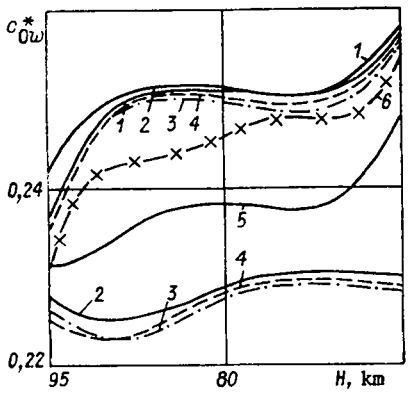

Fig. 3

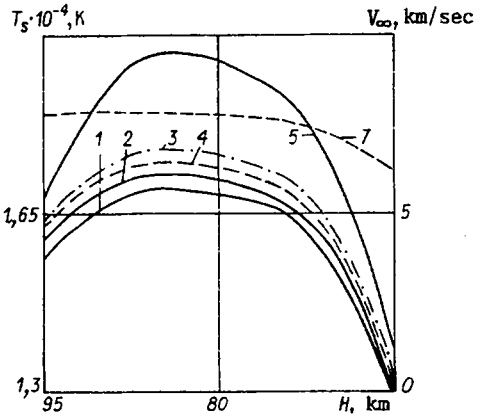

Fig. 4

in concentrations within the shock layer exceeds the value of the diffusion flux on the shockwave boundary. Therefore, the shockwave seems to be a sink for the chemical element O. This occurs because application of the transport equation on the boundary under the fixed boundary condition $c^*_{is} = c^*_{i\infty}$ automatically yields the diffusion flux of the element on it. Conservation laws are utilized in the boundary conditions (1.7) and (1.8) and this diffusion flux is compensated by a reverse convective flux.

Taking account of the barodiffusion in the simplified **Navier—Stokes** equations (the line 3) that causes a redistribution of the chemical components (the lighter N and O atoms are concentrated in the shockwave zone) diminishes the concentration of the element O in the shock layer. In the shockwave domain the influence of barodiffusion on the component and element concentrations significantly predominates over the influence of multicomponent diffusion.

Let us consider the Rankine—Hugoniot relationships for the concentrations on the stagnation line with chemical reactions within the shockwave taken into account

$$c_{is} - c_{i\infty} = I_{is} + J_{is}, \quad J_{is} = \int_{x^3_s}^{\infty} \dot{w}_i dx^3, \quad i = 1, \ldots, N.$$

For the simplified Navier—Stokes equations behind the inner shockwave boundary we take the point x^3_s at which the density profile has the greatest slope. For a more accurate localization of x^3_s several computations are performed for one modification with an insignificantly altered mesh spacing (within the limits of the spacing in the shockwave) so that the shockwave structure was determined by values of the quantities at 30-60 points. Let us note that the maximum temperature is achieved within the shockwave for such a selection of x^3_s.

Values of the component concentrations on the shockwave, obtained as a result of solving the thin viscous shock layer equations (the system II) are given in Fig. 2 by solid lines, c_{is} by dashes, and values of $c_{i\infty} + I_{is}$ obtained during the solution of the simplified Navier—Stokes equations (the system I) without taking account of barodiffusion by dash-dot lines. The difference between the values displayed by the dashed and dash-dot lines determines the integral of the source term.

The integral of the source term is 10-25% of the diffusion flux on the inner shockwave boundary at the 90-65 km section of the trajectory, where chemical reactions are substantial on the shockwave boundary.

At altitudes H < 65 km as the diffusion flux diminishes at the shockwave boundary the relative contribution of the chemical reactions in the shockwave to the quantity c_{is} diminishes simultaneously. For H > 95 km the reactions are frozen in a strongly diffused shockwave and for $x^3 = x^3_s$ the sign of the diffusion flux can be opposite to the sign of $c_{is} - c_{i\infty}$. The sign of I_{is} always agrees with the sign of $c_{is} - c_{i\infty}$ on the shockwave boundary in the thin viscous shock layer model.

For $H \leqslant 95$ km the diffusion flux on the shockwave boundary, obtained during the solution of the system II exceeds in absolute magnitude both the $|I_{is}|$ and the $|I_{is} + J_{is}|$ of

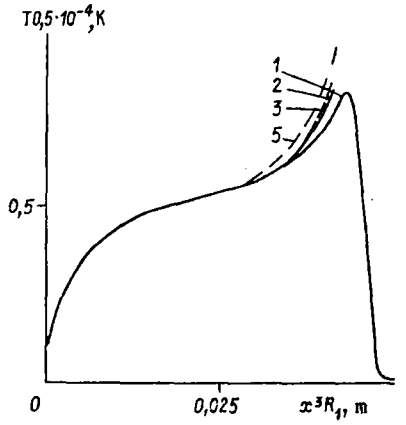

Fig. 5

the system I. The addition of the integral of the source term to the boundary conditions (1.8) of the system II just would increase the difference between the concentrations from the solution of the system I.

The influence of barodiffusion in the system I on the concentration in the shockwave domain is substantially greater than the contribution of the chemical reactions in the absence of barodiffusion. Consequently, examination of the leading shock front structure to take account of the chemical reactions in the boundary conditions for the concentration in the viscous shock layer model is meaningful only when taking account of barodiffusion simultaneously. Let us also note that $|J_{is}|$ increases when barodiffusion is taken into account, but meanwhile the ratio J_{is}/I_{is} can be almost halved.

To estimate the degree of influence of the chemical reactions in the leading shock front on the flow characteristics in the boundary conditions (1.8) of the system II, values of I_{is} and $I_{is} + J_{is}$ from the solution of the system I were substituted in place of the diffusion flux.

The concentration of the element O on the body is represented in Fig. 3 as a function of the flight altitude. Lines 1 and 6 correspond to the solution of the system I without and with the barodiffusion taken into account, 2 is the solution of the system II, and 3-5 are the solution of the system II with values of I_{is}, $I_{is} + J_{is}$, and 0 used in the boundary conditions (1.8) in place of I_i. The three lower curves refer to a non-catalytic surface and the rest to an ideally catalytic surface.

As a result of taking account of the chemical reactions in the shockwave (the term J_{is}) the concentration change on the body surface is significantly less than the concentration change with barodiffusion taken into account in the system I. Application of the ordinary Rankine—Hugoniot relationships results in substantial error in the element constitution on the surface.

The temperature on the shockwave boundary is shown in Fig. 4 as a function of the flight altitude while the temperature profiles for H = 75 km is displayed in Fig. 5 for an ideally catalytic surface. The line notations agree with Fig. 3. The change in boundary conditions for the concentration results in a change in the temperature profile mainly in just the domain abutting on the shockwave. In practice barodiffusion exerts no influence on the temperature profile.

The heat flux to the body surface consists of the sum of the convective and the chemical components

$$q = q_k + q_x, \quad q_k = \frac{\mu c_p}{\sigma \mathrm{Re}_\infty} \frac{\partial T}{\partial x^3}, \quad q_x = -\sum_{i=1}^{N} h_i I_i.$$

As the concentration on the shockwave boundary changes in the case of a catalytic surface, both components vary but to opposite sides. The final change q_x grows as the altitude increases and q_x at $H \geqslant 95$ km can be different by several times. But the degree of dissociation in the upper part of the trajectory is insignificant because of the low density of

the incoming stream and the contribution of q_x to the heat flux is slight. As the altitude decreases to H ∿ 95-90 km the change in q_k increases and then diminishes. The greatest difference in the heat fluxes is achieved at H ∿ 95-90 km altitudes, where the flow mode corresponds to a diffuse layer with a considerable degree of dissociation.

Thus for an ideally catalytic surface the difference in the heat flux when taking account of the chemical reactions in the shockwave (utilization of the values of $I_{is} + J_{is}$ in contrast to I_{is} in the boundary condition (1.8)) are the following: q_k is 1.3% less, q_x is 12% greater, and the total flux q is just 0.1% greater. As an inviscid flow zone forms the concentration change on the shockwave is not felt in practice in the magnitude of the heat flux and at $H \leqslant 75$ km altitudes the heat flux increases by less than 0.003% in the case mentioned above.

For a non-catalytic surface $q_x = 0$ and the maximal diminution of the heat flux is 1.1% for H = 95 km. Taking account of chemical reactions in the shockwave, the difference in the heat flux does not exceed 1% when using the model [13] of catalytic activity of the surface in which the recombination constants depend on the temperature.

Application of the ordinary Rankine—Hugoniot relationships for the concentration in contrast to conditions (1.7) and (1.8) changes the heat flux to a greater degree. For an ideally catalytic surface in the H = 110-50 km range the maximal difference is achieved at H = 90 km: q_k is 10.7% greater, q_x is 58% less, and q diminishes by just 0.8%. For a non-catalytic surface q is 11.6% greater for H = 95 km while the difference does not exceed 1% for $H \leqslant 75$ km.

Taking account of the chemical reactions in the shockwave diminishes the friction coefficient for an ideally catalytic surface up to 0.2% while up to 0.35% for a non-catalytic surface. Utilization of the ordinary Rankine—Hugoniot relationships for the concentration increases the friction coefficient up to 1.6% for a catalytic surface and up to 3.5% for a noncatalytic surface. The maximal change in the friction coefficients is achieved at H = 95-90 km while the friction coefficients practically agree for $H \leqslant 75$ km.

Taking account of barodiffusion in the simplified Navier—Stokes equations diminishes the heat flux by not more than 2% and changes the friction coefficients by not more than 0.3%.

The heat flux obtained in the solution of the system II exceeds the solution of the system II by not more than 4% at the altitudes $65 \leqslant H \leqslant 90$ km, while the friction coefficients agree to 1% accuracy.

In conclusion, the deduction can be made that the assumption of freezing of the chemical reactions in the shockwave results in a smaller error in the determination of the concentration, heat flux, and friction coefficient fields than does neglecting the barodiffusion effects. Neglecting chemical reactions in the shockwave is justified when determining the heat flux and the friction coefficients during motion over a glide trajectory (the maximal error in determining the heat flux is on the order of 1%). At altitudes where an inviscid flow domain was formed the heat flux is practically independent of the boundary conditions for the concentrations at the shockwave.

The author is grateful to G. A. Tirskii for constant attention to the research.

LITERATURE CITED

1. H. K. Cheng, "Hypersonic shock-layer theory of the stagnation region at low Reynolds number," Proc. Heat Transfer and Fluid Mech. Inst., Stanford (1961).
2. H. K. Cheng, "The blunt body problem in hypersonic flow at low Reynolds number," J. Astronaut. Sci., No. 92 (1963).
3. L. I. Sedov, M. P. Mikhailova and G. G. Chernyi, "On the influence of viscosity and heat conductivity on gas flow behind a strongly curved shockwave," Vestn. Mosk. Gos. Univ., Ser. Fiz.-Mat. Nauk, No. 3 (1953).
4. G. N. Zalogin and V. V. Lunev, "On the model of a viscous nonequilibrium shock layer with a thin shockwave," Izv. Akad. Nauk SSSR, Mekh. Zhidk. Gaza, No. 5 (1973).
5. A. S. Gorinov and K. M. Magomedov, "Method of splitting for the solution of relaxation equations in the presence of diffusion," Zh. Vychisl. Mat. Mat. Fiz., 13, No. 5 (1973).

6. É. A. Gershbein, "Asymptotic investigation of the problem of spatial hypersonic viscous gas flow around blunt bodies with a permeable surface," Hypersonic Spatial Flow in the Presence of Physicochemical Transformations [in Russian], Moscow (1981).
7. É. A. Gershbein, V. S. Shchelin, and S. A. Yunitskii, "Investigation of the spatial flow around bodies with a catalytic surface during their motion in earth's atmosphere," Kosm. Issled., No. 3 (1985).
8. G. A. Tirskii, "On the theory of hypersonic flow around plane and axisymmetric blunt bodies by a viscous chemically reacting gas in the presence of blowing," Tr. Inst. Mekh., Mosk. Gos. Univ. [in Russian], No. 39 (1975).
9. É. A. Gershbein and V. G. Shcherbak, "Investigation of hypersonic spatial flow around blunt bodies within the framework of parabolized Navier—Stokes equations," Izv. Akad. Nauk SSSR, Mekh. Zhidk. Gaza, No. 4 (1987).
10. H. C. Kao, "Hypersonic viscous flow near the stagnation streamline of a blunt body," AIAA J., 2, No. 11 (1964).
11. I. V. Petukhov, "Numerical analysis of two-dimensional flows in the boundary layer," Numerical Methods of Solving Differential and Integral Equations and Quadrature Formulas [in Russian], Moscow (1964).
12. R. V. Masek, D. Hender, and J. A. Forney, "Evaluation of aerodynamic uncertainties for the space shuttle," AIAA Paper No. 737, New York (1978).
13. C. D. Scott, "Catalytic recombination of nitrogen and oxygen on high-temperature reusable insulation," AIAA Paper No. 1477, New York (1980).

SPATIAL DISTRIBUTION OF CO_2 DIMERS IN AXISYMMETRIC GAS JETS EXPANDING IN A VACUUM

A. A. Vigasin and V. N. Makarov

UDC 533.17;539.196.3

The condensation of molecular gases in engines and in laser and gas-dynamical equipment has attracted the attention of researchers for decades. However the capability of gases expanding in a vacuum to associate has been actively used only in recent years to study the earliest stages of this process and the weak molecular interactions leading to the formation of van der Waals or hydrogen-bonded complexes. These studies were based on special methods of microwave and optical spectroscopy. The use of spectroscopic methods in combination with the gas-dynamical method of generating molecular complexes has been used to obtain extensive information on the structure and properties of complexes (see [1], for example). But the further development and increased sensitivity of the spectroscopic methods of probing gas flows requires in many cases a more detailed theoretical description of the physical and chemical processes in nonequilibrium moving media. In particular, for experiments designed to obtain spectra of molecular complexes of certain compositions and sizes, a careful consideration of the optimal choice of the geometrical and other parameters is usually necessary.

The kinetics of the initial stages of the condensation—dimerization of molecular gases such as water vapor and carbon dioxide has been studied by several authors [2-7]. However these studies were concerned mainly with determining the dependence of the steady-state concentration of dimers in a molecular beam on the parameters in the mixing chamber and on the nozzle diameter. The fraction of dimers was measured in [2-4] with a mass spectrometer and the composition of the gas was controlled only along the direction of propagation of the molecular beam.

Spectroscopic studies of the rotational and vibrational—rotational transitions of complexes are usually carried out under conditions such that the probing beam (or beams) of electromagnetic radiation pass through a jet of freely expanding gas in the direction perpendicular to the symmetry axis of the jet. This geometry is also typical of the widely-used method of microwave Fourier spectroscopy, and in the study of infrared absorption and spontaneous and coherent anti-Stokes Raman scattering [1]. In the design of experiments of this kind it is desired to have an idea of the spatial distribution of dimers in the expanding

Moscow. Translated from Zhurnal Prikladnoi Mekhaniki i Tekhnicheskoi Fiziki, No. 1, pp. 56-62, January-February, 1989. Original article submitted October 22, 1987.

 0021-8944/89/3001-0052$12.50